

Experimental and Theoretical Study of the Surface Tension in Liquid Ag–Cu–Sn Alloys

Ivan G. Kaban, Sascha Gruner, and Walter Hoyer*

Institute of Physics, Chemnitz University of Technology, D-09107 Chemnitz, Germany

Received September 12, 2004; accepted November 9, 2004
Published online November 14, 2005 © Springer-Verlag 2005

Summary. The surface tension in the ternary Ag–Cu–Sn system in a wide composition and temperature range has been determined experimentally. Besides, the surface tension of the investigated alloys has been modeled using the theoretical approach of *Butler*. The measured and the calculated absolute values of the surface tension are compared and analyzed.

Keywords. Ag–Cu–Sn alloys; Surface energy; Thermodynamics.

Introduction

Recently the Ag–Cu–Sn system came in sight of the applied science following a search of a lead-free solder material being capable to substitute for traditional Pb–Sn solders. Therefore, a systematic study of various physical properties of solid as well as liquid Ag–Cu–Sn alloys is required. Because of the crucial role of the wetting in soldering process, knowledge of the surface tension of liquid Ag–Cu–Sn alloys is of a high importance. In this work we report the experimental data on the surface tension in ternary Ag–Cu–Sn melts. Besides, the surface tension for the investigated alloys is calculated using the absolute values of the surface tension of pure components and the thermodynamic characteristics of the binary Ag–Cu, Ag–Sn, and Cu–Sn systems.

Results and Discussion

In order to study the behavior of the surface tension in liquid Ag–Cu–Sn system in dependence on temperature and composition, the alloys from the line Sn–Ag₇Cu₃ lying in the vicinity of ternary eutectic line in the Ag–Cu–Sn system [1] have been chosen. Figure 1 shows the experimental temperature dependences of the surface

* Corresponding author. E-mail: hoyer@physik.tu-chemnitz.de

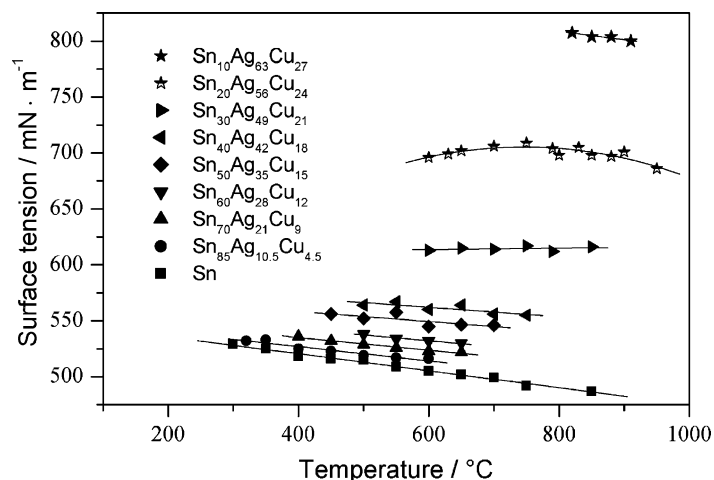


Fig. 1. The temperature dependences of the surface tension in liquid Ag–Cu–Sn alloys; the lines are guides for the eye

tension σ as well as the compositions of the investigated alloys. The temperature dependences of σ are not of the same character for all investigated alloys, and the temperature behavior depends on the alloy composition. In the studied temperature intervals, the surface tension of $(\text{Ag}_7\text{Cu}_3)_{100-x}\text{Sn}_x$ alloys with $40 \leq x \leq 100$ decreases with increasing temperature. The surface tension of the $\text{Sn}_{30}\text{Ag}_{49}\text{Cu}_{21}$ alloy in the temperature interval 600–850°C exhibits virtually no temperature dependence. The surface tension of the $\text{Sn}_{20}\text{Ag}_{56}\text{Cu}_{24}$ alloy firstly increases with temperature and then it decreases when the temperature is farther increasing. For the alloy containing 10 at.% Sn it is difficult to make any conclusion because of the short temperature interval studied.

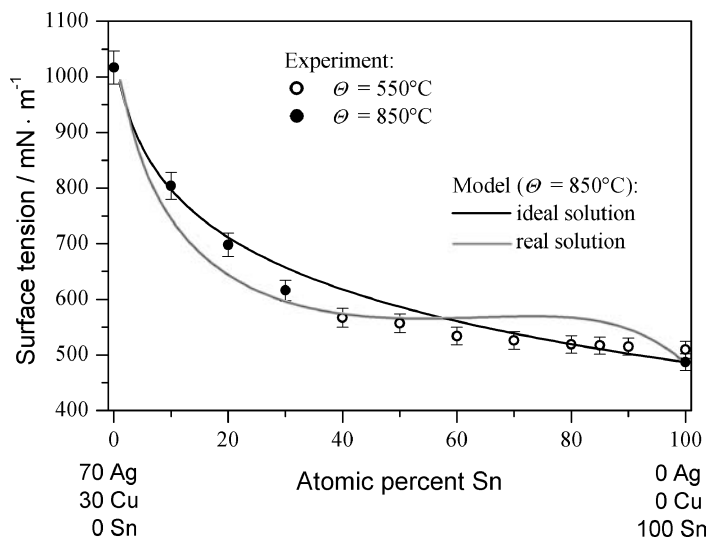


Fig. 2. The composition dependences of the surface tension in the $(\text{Ag}_7\text{Cu}_3)_{100-x}\text{Sn}_x$ alloys; symbols: experimental data; lines: theoretical calculations

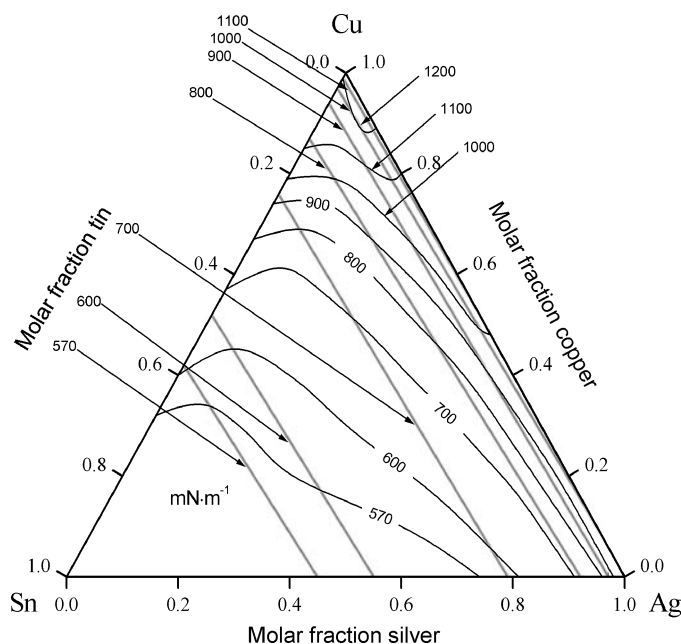


Fig. 3. The calculated surface tension contours for liquid Ag–Cu–Sn alloys at 850°C; black lines: real solutions; light lines: ideal solutions; the absolute values of the surface tension are given in $\text{mN} \cdot \text{m}^{-1}$

The isothermal composition dependences of σ along the line Sn–Ag₇Cu₃ are plotted in Fig. 2. The surface tension varies very weakly with composition when Sn content is higher than 80 at.%. Noticeable changes are observed when concentration of Sn in ternary alloys becomes less than ~70%.

Figure 3 shows the surface tension contours in the Ag–Cu–Sn alloys at $\vartheta = 850^\circ\text{C}$ calculated with the theoretical approach of *Butler*. The model of ideal solutions gives straight lines of constant σ that go nearly parallel to the Ag–Cu binary line. The surface tension contours obtained with the model of real solutions are curved lines over the whole concentration triangle.

For a better comparison, the calculated values of the surface tension at $\vartheta = 850^\circ\text{C}$ along the line Sn–Ag₇Cu₃ are shown in Fig. 2 together with the experimental data. Both models yield the surface tension rapidly decreasing with small additions of Sn and weakly changing at the Sn-rich side. The highest deviation of the calculated values from the experimental results is ~12% for the model of ideal solutions and ~16% for the model of real solutions. It is to be noted that the surface tension calculated with the model of ideal solutions decreases gradually with increasing Sn content over the whole composition range, whereas the application of the real solutions approximation leads to a hump at about 70–80 at.% of Sn. Obviously this increase is connected with the Ag–Sn part of the thermodynamic data, since the theoretical values of σ calculated with the model of real solutions for binary Ag–Sn alloys show a similar hump on the Sn-rich side.

Figure 4 presents the temperature dependences of the surface tension $\sigma(\vartheta)$ for the (Ag₇Cu₃)_{100-x}Sn_x alloys determined with the approximations of ideal and real solutions. In general, both models reproduce the temperature behavior of σ

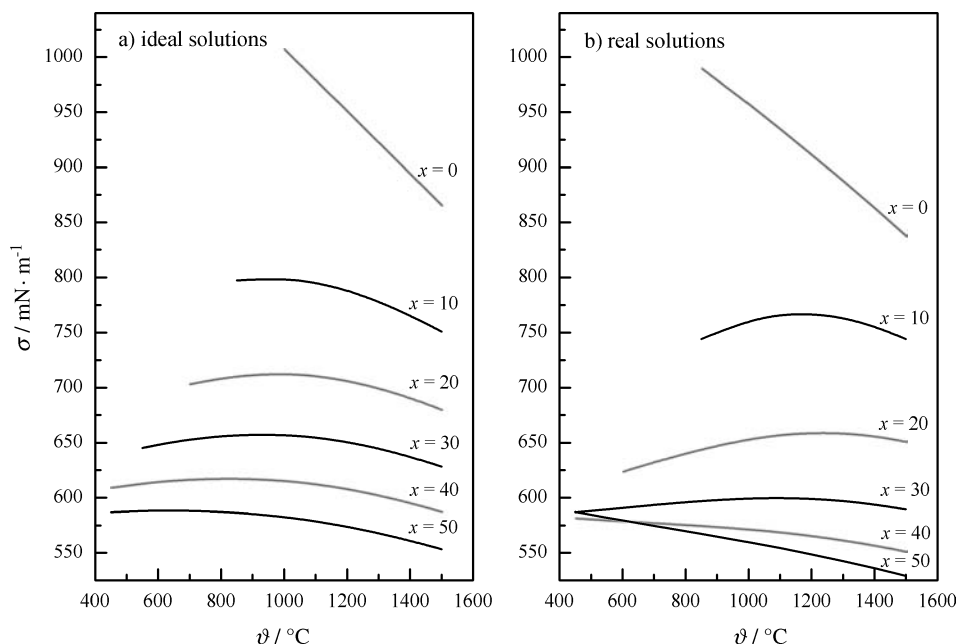


Fig. 4. The simulated temperature dependences of the surface tension for the $(\text{Ag}_7\text{Cu}_3)_{100-x}\text{Sn}_x$ alloys

established experimentally: i) the surface tension of Sn-rich alloys (>40 – 50 at.% Sn) exhibits negative temperature dependences over the whole temperature range studied theoretically; ii) the surface tension of the alloys containing <30 – 40 at.% Sn shows positive temperature dependences at low temperatures and negative ones at high temperatures. However the temperature dependences of σ determined with the approximation of real solutions seem to be closer to the experimental results shown in Fig. 1. This is well seen from comparison of the theoretical and the experimental temperature dependences for the alloys containing 20 and 30 at.% Sn.

Prasad and Mikula [2] have studied the surface tension in the Cu–Sn liquid alloys and found a positive temperature coefficient for $\sigma(\vartheta)$ at 75 at.% Cu and zero coefficient around the equiatomic composition. They suggested that such behavior is connected with compound formation tendencies and dissociation at the surface of atomic clusters associated with the γ -phase of the Cu–Sn system. Obviously different types of the temperature dependences $\sigma(\vartheta)$ for the $(\text{Ag}_7\text{Cu}_3)_{100-x}\text{Sn}_x$ alloys are also related with formation (by decreasing temperature) or disintegration (by increasing temperature) of atomic clusters corresponding to the Ag–Sn and Cu–Sn compounds in the solid Ag–Cu–Sn alloys and variation of the Sn-content in the bulk and in the surface phases.

Conclusions

It has been established experimentally that the temperature behavior of the surface tension of ternary $(\text{Ag}_7\text{Cu}_3)_{100-x}\text{Sn}_x$ alloys depends on the Sn content: i) the surface tension shows negative temperature dependences over the whole temperature range for $x \geq 40$; ii) $d\sigma/dT \approx 0$ for $x = 30$; iii) σ shows a positive temperature

dependence at low temperatures and a negative one at high temperatures for $x = 20$. The theoretical approach of *Butler* yields a similar temperature behavior both with model of ideal and model of real solutions. However, the shape of the curves $\sigma(\vartheta)$ simulated with the model of real solutions is closer to the experimental results. The composition dependences of σ calculated with the approximation of ideal solutions decreases gradually with increasing Sn content in agreement with the experimental data, whereas there appears a hump on the calculated curves at the Sn-rich side when the model of real solutions is applied.

Methods

Experimental

The measurement technique [3] is based on the experimental measurement of the force exerting on the alumina stamp submerged below the level of the free liquid surface. Application of the cylindrical stamp allows investigation of the meniscus formation and contraction up to the complete tearing of the stamp away from the surface. After correction of the experimental data for buoyancy force and geometry of the crucible and the stamp, the volume of the meniscus in dependence on the height of the contact line is determined. On the other hand, the meniscus is modeled by the numerical solution of *Laplace's* equation for different values of the capillary constant. From the simulated meniscus curves the meniscus volumes can be calculated. Then the experimental and theoretical volume curves are compared and the capillary constant is calculated. For the calculation of the surface tension the density is determined from the buoyancy force exerted by the liquid sample on the stamp immersed into it.

The measurements have been performed in a vertical high temperature chamber (1 m length, 0.1 m inner diameter). Before heating the chamber was evacuated to better than $5 \cdot 10^{-5}$ m bar and then filled with a gas mixture of Ar-10% H₂ with a total pressure of ~ 1 bar. The graphite crucible (5 cm inner diameter, 4 cm height) was moved by an ultrahigh vacuum manipulating system. The weight of the stamp was measured by a balance with an accuracy of ± 1 mg. The experimental error did not exceed 3% for the surface tension and 1.5% for the density.

The samples were prepared from granules of Ag (99.99), Cu (99.999), and Sn (99.99).

Theoretical

The surface tension in liquid binary as well as ternary alloys can be estimated using *Butler's* equation (Eq. (1)) [4]

$$\sigma = \sigma_i + \frac{RT}{S_i} \ln \left(\frac{\hat{x}_i}{x_i} \right) + \frac{1}{S_i} \left(\Delta^{XS} \hat{G}_i - \Delta^{XS} G_i \right). \quad (1)$$

Here T is the absolute temperature; R the gas constant; the subscript i denotes the components of the alloy; σ_i the surface tension of pure components; S_i the surface area of the i th component, which can be calculated as $S_i = f \cdot N_A^{1/3} \cdot V_i^{2/3}$ with *Avogadro's* number N_A , component's molar volume V_i , and geometry factor $f = 1.091$ for a dense packing. The x_i and \hat{x}_i give the molar fraction of a compo-

Table 1. Optimized *Redlich-Kister* coefficients for binary Ag–Sn, Ag–Cu, and Cu–Sn systems

System	$L_0/\text{J} \cdot \text{mol}^{-1}$	$L_1/\text{J} \cdot \text{mol}^{-1}$	$L_2/\text{J} \cdot \text{mol}^{-1}$
Ag–Sn [6]	$-4902.5 - 4.30532T$	$16474.0 - 3.12507T$	-7298.6
Cu–Sn [7]	$-9002.8 - 5.8381T$	$-20100.5 + 3.6366T$	-10528.4
Ag–Cu [8]	$17323.4 - 4.46819T$	$1654.38 - 2.35285T$	0.0

ment i in the bulk and in the surface layer, respectively. The $\Delta^{XS}G_i$ and $\Delta^{XS}\widehat{G}_i$ are the partial molar excess *Gibbs* energies of the i th component in the bulk phase and in the surface layer.

Two thermodynamic approximations were applied: i) model of ideal solutions, where the excess *Gibbs* energy is zero; ii) model of real solutions, where optimized excess *Gibbs* energies in terms of *Redlich-Kister* polynomials (Eq. (2)) [5] were used to introduce a “real” thermodynamic behavior of the studied alloys.

$$\Delta^{XS}G = x_1x_2 \sum_i L_i(x_1 - x_2)^i \quad (2)$$

The excess *Gibbs* energies for the ternary alloys were calculated as the sums of those for the binary alloys, and the ternary contributions were neglected. The polynomial coefficients L_i for the binary Ag–Sn, Ag–Cu, and Cu–Sn systems taken from Refs. [6–8] are given in Table 1.

It is assumed that $\Delta^{XS}G_i$ and $\Delta^{XS}\widehat{G}_i$ can be given by the same Eq. (2), but they differ due to various compositions of the bulk and the surface phase. It is suggested in the literature that a difference between the coordination number N in the bulk and the coordination number \widehat{N} in the surface phase has also to be considered, so that $\Delta^{XS}\widehat{G}_i = \widehat{N}/N \cdot \Delta^{XS}G_i$ with $0.5 \leq \widehat{N}/N \leq 1.0$ (e.g., see Ref. [9] for a review). In the present work $\widehat{N}/N = 1.0$ is applied.

The surface tension of pure Ag and Cu used in the calculations was taken from Ref. [10]: $\sigma_{\text{Ag}} = (1252 - 0.31T) \text{ mN} \cdot \text{m}^{-1}$, $\sigma_{\text{Cu}} = (1656 - 0.26T) \text{ mN} \cdot \text{m}^{-1}$. The surface tension of pure Sn was determined in the present work: $\sigma_{\text{Sn}} = (572 - 76 \cdot 10^{-3}T) \text{ mN} \cdot \text{m}^{-1}$.

References

- [1] Petzow G, Effenberg G (eds) (1988) Ternary Alloys, vol 2. VCH Verlagsgesellschaft, Weinheim, p 38
- [2] Prasad LC, Mikula AJ (2001) *J Alloys Comp* **314**: 193
- [3] Merkwitz M (1997) PhD Thesis, Chemnitz University of Technology, <http://archiv.tu-chemnitz.de/pub/1997/0036>
- [4] Butler JAV (1932) *Proc Roy Soc A* **135**: 348
- [5] Redlich O, Kister AT (1948) *Ind Eng Chem* **40**: 345
- [6] Kattner UR, Boettinger WJ (1994) *J Electron Mater* **23**: 603
- [7] Shim JH, Oh CS, Lee BJ, Lee DN (1996) *Z Metallkd* **87**: 205
- [8] Moon KW, Boettinger WJ, Kattner UR, Biancaniello FS, Handwerker CA (2000) *J Electron Mater* **29**: 1122
- [9] Tanaka T, Iida T (1994) *Steel Res* **65**: 21
- [10] Keene BJ (1993) *Int Mat Rev* **38**: 157